J Mater Sci (2006) 41:5371–5375
DOI 10.1007/s10853-006-0407-y

LETTER

Morphology and orientation of the equilibrated Au–sapphire $(10\bar{1}0)$ interface

Hila Sadan · Wayne D. Kaplan

Received: 21 March 2006 / Accepted: 1 May 2006 / Published online: 1 August 2006
© Springer Science+Business Media, LLC 2006

Metal–sapphire (α-Al_2O_3) interfaces have been the focus of basic studies in the investigation of metal–ceramic interfaces [1–8]. The surface energy of low index planes in sapphire was extensively studied in the last decade, by analyzing the equilibrium shape (Wulff shape) of cavities equilibrated at relatively high temperatures [9, 10]. It was found that the low energy planes (facets) at 1,600 and 1,800 °C in air and vacuum are: the C-plane {0001}, the R-plane $\{10\bar{1}2\}$, the A-plane $\{1\bar{2}10\}$, the P-plane $\{11\bar{2}3\}$ and the S-plane $\{10\bar{1}1\}$ [11, 12]. The prismatic (M-plane) $\{10\bar{1}0\}$ was not experimentally observed [13], although it was theoretically predicted to be a low energy plane [14].

The tendency of the sapphire M-plane to break-up and form a hill-and-valley surface morphology was reported for both the free surface, and the sapphire–anorthite glass interface [15, 16]. The facets composing the hill-and-valley surface morphology of the decomposed M-plane were identified as $\{1\bar{1}02\}$ and $\{10\bar{1}1\}$ intersecting along a $< 11\bar{2}0>$ direction [15–22]. In addition, facet junctions were identified, defining regions of curved surfaces [21, 23]. While the details of the equilibration of the unique hill-and-valley morphology which forms on the M-plane are often ignored, the rather unique geometry of this surface is often used for controlled nucleation and growth during gas phase deposition [15, 24–27]. In the present study, the microstructure and morphology of the interface between faceted M-plane sapphire and equilibrated Au particles was examined.

H. Sadan · W. D. Kaplan (✉)
Department of Materials Engineering, Technion – Israel Institute of Technology, Haifa 32000, Israel
e-mail: kaplan@tx.technion.ac.il

$(10\bar{1}0)$-oriented sapphire (α-Al_2O_3) substrates of 99.99% purity (Gavish Industrial Technologies & Materials) were ultrasonically cleaned in acetone and ethanol, and annealed for 2 h at 1,200 °C in air. At this stage, a regular array of facets was formed instead of the less thermodynamically stable prismatic surface. A ~20 nm thick Au film was deposited on the substrates using a Polaron sputter coater. The specimens were annealed in air at 1,100 °C for 30 min. Since at this temperature Au is liquid (T_m = 1,064 °C), dewetting of the film occurred due to the finite contact angle of liquid Au with sapphire [28]. This resulted in an extremely large number of sub-micron droplets [29, 30]. Specimens were then cooled to 1,000 °C (0.95 T_m) and annealed in air for various durations of time (0.5, 5, 10, 20, 50 and 100 h) in order to reach equilibrium. This process resulted in faceted particles with diameters varying from 100 to 900 nm (see Fig. 1).

Initial examination of the specimens was conducted using high resolution scanning electron microscopy (HRSEM) on a LEO 982 Gemini microscope equipped with a field emission gun (FEG–SEM). Pronounced unidirectional faceting of the substrate was observed, containing a relatively large density of junctions and discontinuities. Morphological examination of the equilibrated particles was conducted to identify any preferred orientation, which would indicate a low-energy configuration corresponding to a minimum in interfacial energy versus particle orienation [31–33]. It was observed that ~50% of the particles had a similar equilibrium shape. In addition, it was found that these particles were aligned approximately ±27° with respect to the facets on the substrate, which indicates that there is an orientation relationship between Au and M-plane sapphire (see Fig. 2).

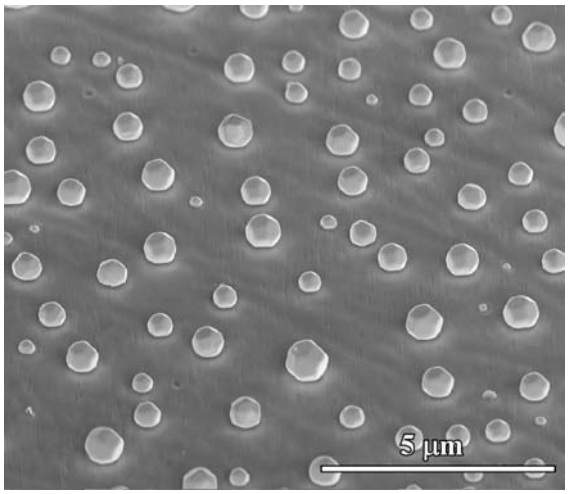

Fig. 1 Secondary electron SEM micrograph of Au particles equilibrated on a ($10\bar{1}0$) sapphire substrate at 1,000 °C for 100 h. The micrograph was acquired at a 52° tilt with respect to the substrate normal

To determine the preferred orientation of the particles identified in Fig. 2, electron backscattered diffraction (EBSD) patterns were acquired and indexed using a Link Opal EBSD System (Oxford Instruments, UK) [34], mounted on the HRSEM. EBSD measurements were conducted at 20 kV with a ~3 nA electron-probe current, at a 20 mm working distance. EBSD measurements were acquired from 20 different particles from each sample (equilibrated at different times at 1,000 °C). The time required for equilibrium was estimated as the time after which no significant change was detected in the particle orientation relative to the substrate. The results are presented in Fig. 3.

The results show the existence of a preferred orientation of 58% of all examined particles. The fact that no significant change in the orientation of the particles

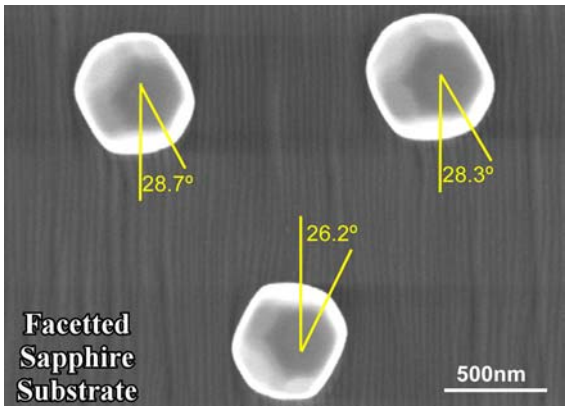

Fig. 2 Secondary electron SEM micrograph of three Au particles with a similar morphology, equilibrated on the facetted sapphire substrate at 1,000°C for 100 h. All of the particles are rotated approximately 27° with respect to the facets

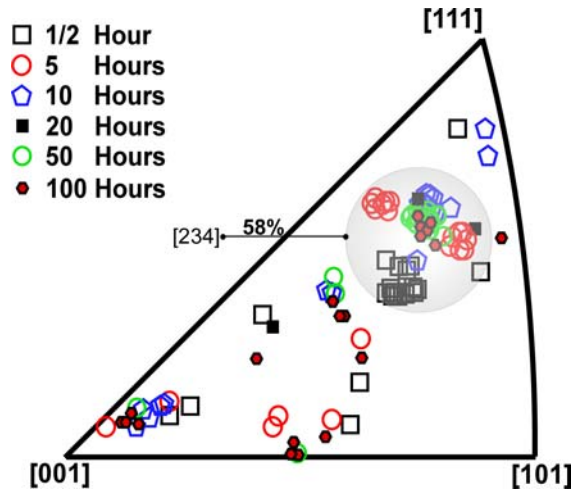

Fig. 3 Inverse pole figure from Au particles, dewetted on the sapphire substrates at 1000°C as a function of time (data from EBSD-SEM). Twenty particles were characterized for each annealing time, except for the sample equilibrated for 20 h, for which three particles were characterized

was detected as a function of annealing time indicates that the orientation was determined at the nucleation stage of the particle. It should be noted that the information regarding the orientation of the particle, acquired by EBSD, provides information from no more than 40 nm below the surface of the particle [35]. This information can be used to determine the particle orientation providing grain boundaries do not delimit the top facet from the interface. A small deviation in the normal of the particles from the [234] direction can be observed in Fig. 3. The estimated accuracy of the measurement is ±2°, including the systematic error in alignment of the SEM stage after exchanging each specimen, which accounts for this deviation. All of the following will focus only on the particles with the morphology identified in Fig. 2, which correlates to the particles oriented with the [234] normal to the sapphire surface (58% of the total number of investigated particles).

Focused ion beam (FIB – FEI Strata 400s) cross-sections were made in several particles (identified to have the [234] direction normal to the sapphire surface) to examine the interface morphology and search for grain boundaries. All of the cross-sections revealed at least one of the two grain boundaries seen in Fig. 4, even after 100 h at 1,000 °C. In addition, it was confirmed that the equilibrium shape of the particles did not contain any facet, which is parallel to the original $(10\bar{1}0)$ sapphire surface. A combination of the orientation of the particles determined by EBSD and geometrical analysis of the cross-sections revealed that all three surface facets of the large grain indicated in Fig. 4 are {111} planes. In addition, it was found that

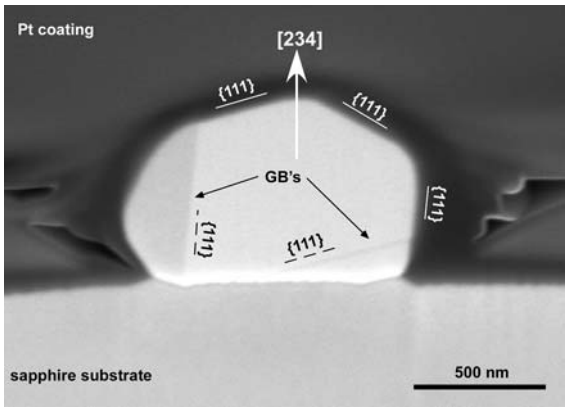

Fig. 4 Secondary electron SEM micrograph of a particle cross-sectioned using the FIB. Two grain boundaries (GB's) are visible

both grain boundaries are parallel to {111} planes with respect to the large central grain.

While EBSD was used to determine the preferred orientation of the Au particles with respect to the substrate, selected area electron diffraction (SAD) and transmission electron microscopy (TEM–JEOL 3010 UHR, operated at 300 kV and with a point resolution better than 0.16 nm) was used to examine the orientation relationship and the morphology of the interface. TEM specimens were prepared from the center of particles with the morphologies shown in Fig. 2, using the ''lift out'' technique in the FIB [36, 37]. Bright field diffraction contrast TEM micrographs and SAD patterns of two particles with the morphology seen in Fig. 2 are presented in Fig. 5.

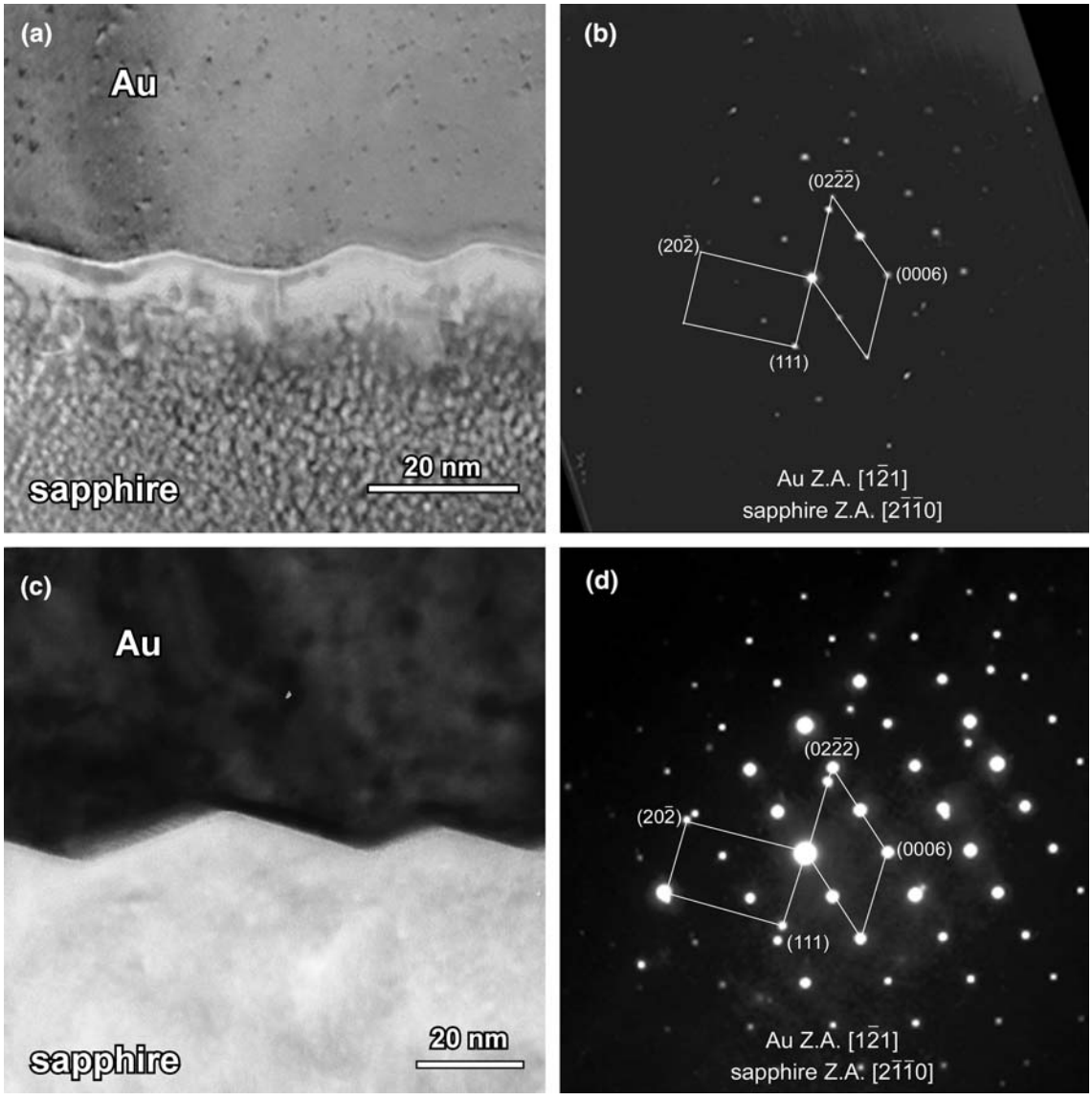

Fig. 5 Bright field TEM micrographs (**a**, **c**) and SAD patterns (**b**, **d**) of Au particles on the sapphire substrate. The samples were prepared from particles with the morphology shown in Fig. 2. Kikuchi electron diffraction was used to orient the substrate in the [2$\bar{1}\bar{1}$0] zone-axis, prior to acquiring the SAD patterns

Although the two particles in Fig. 5 have the same orientation relationship (Au[$1\bar{2}1$]||sapphire[$2\bar{1}\bar{1}0$] and Au(111)||sapphire($0\bar{2}22$)), a variance was found in the interface planes. In both specimens, one interface facet was parallel to Au {111} and sapphire {$0\bar{1}11$}. Since in Fig. 5a both facets are parallel to the incident electron beam (edge-on), the second facet plane could be easily determined, and was found to be composed of sapphire {$01\bar{1}1$} planes. In Fig. 5c one of the facets is not edge-on. Under the assumption that this is a flat facet, trace analysis was used to identify it as the A-plane {$11\bar{2}0$}. Due to the hill-and-valley morphology, at least two different interface planes are formed. It is assumed that the nucleation of the solid Au particle occurred on the {$01\bar{1}\bar{1}$} sapphire surface, since this interface orientation was present in *both* of the examined particles.

Electron diffraction was also used to investigate the facets on the sapphire free-surface (see Fig. 6). It was found that two of the sapphire surface facets are the S-plane ($0\bar{1}11$) and the R-plane ($0\bar{1}1\bar{2}$). The nature of the facets at the free surface of the sapphire are the same as reported in previous works, regarding both the sapphire free surface and the sapphire-anorthite glass interface [15–22]. Figure 7 illustrates the preferred orientation of the particles as determined by EBSD, the orientation relationship and interface/surface planes as determined by TEM.

In summary, an equilibrated orientation relationship between Au and ($10\bar{1}0$) sapphire was determined to be Au(111)||sapphire($01\bar{1}\bar{1}$) and Au[$1\bar{2}1$]||sapphire[$2\bar{1}\bar{1}0$]. It was found that the interface contains more than two facets, probably due to the presence of facet junctions.

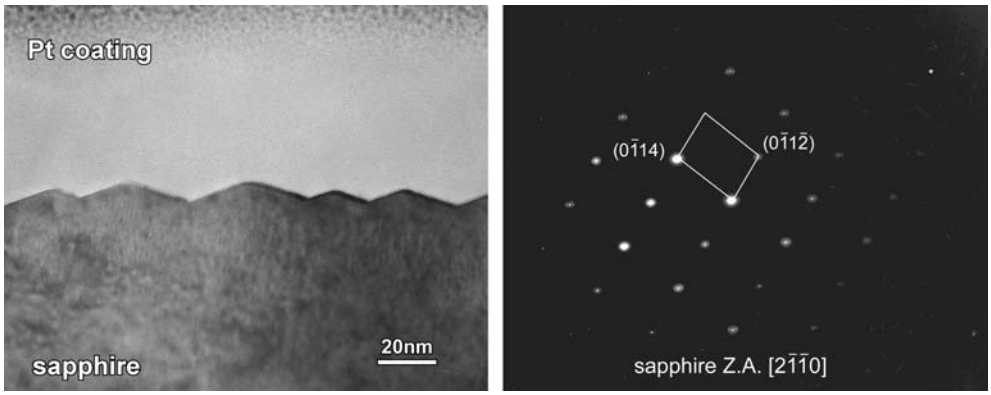

Fig. 6 Bright field TEM micrograph and SAD pattern of a sapphire free surface. Prior to FIB specimen preparation, the surface was protected with a thin layer of Pt by electron beam deposition in the FIB [37]. Kikuchi electron diffraction was used to orient the substrate in the [$2\bar{1}\bar{1}0$] zone-axis, prior to acquiring the SAD pattern. The sapphire surface is composed of ($0\bar{1}11$) and ($0\bar{1}1\bar{2}$) planes

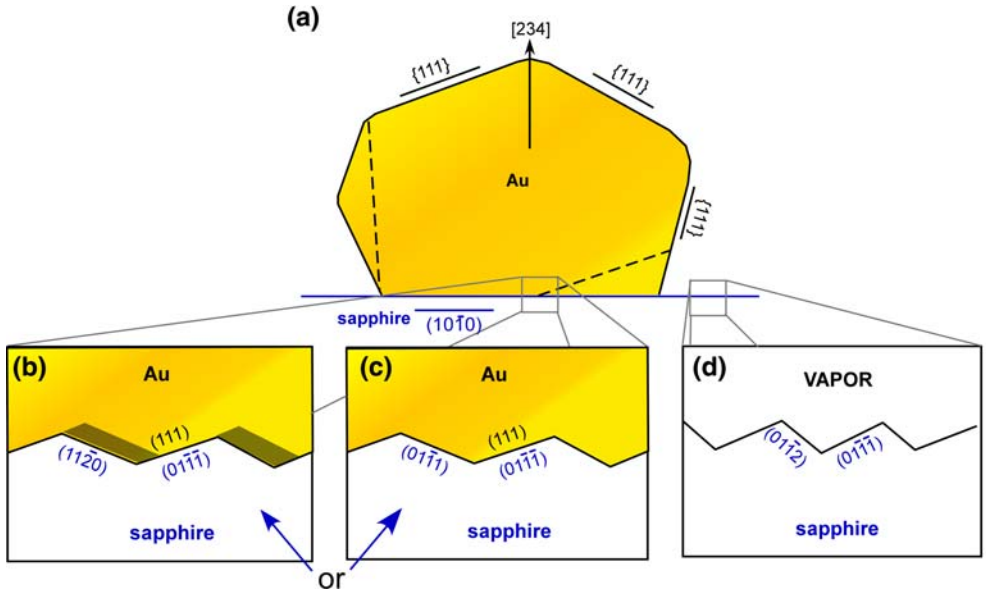

Fig. 7 Orientation relationship and interface/surface facets: (**a**) determined from EBSD and determined from electron diffraction for the interface (**b**, **c**) and sapphire free surface (**c**). Note that one of the interface facets in (**b**) is not 'edge-on'

Two different planes were identified as the second sapphire interface facet: ($01\bar{1}1$) and ($11\bar{2}0$). These planes were not observed in previous investigations of the surface of the M-plane. Furthermore, the $\{01\bar{1}1\}$ plane does not appear in the Wulff shape of sapphire, and is probably stabilized by the interface with Au. It should be noted that while EBSD provides better statistics than TEM, EBSD does not provide complete information on the orientation relationship and the details of the (presumably low energy) interface planes.

Acknowledgements The authors thank D. Chatain, P. Wynblatt, and D. Brandon for enlightening discussions. This research was partially supported by the Israel Science Foundation (#163/05) and the Russell Berrie Nanotechnology Institute at the Technion.

References

1. Rühle M, (1996) J Eur Ceram Soc 16:353
2. Lipkin DM, Clarke DR, Evans AG (1998) Acta Mater 46:4835
3. Levi G, Scheu C, Kaplan WD (2001) Interf Sci 9:213
4. Levi G, Kaplan WD (2002) Acta Mater 50:75
5. Saiz E, Tomsia AP, Suganuma K (2003) J Eur Ceram Soc 23:2787
6. Chatain D, Ghetta V, Wynblatt P (2004) Interf Sci 12:7
7. Avishai A, Scheu C, Kaplan WD (2005) Acta Mater 53:1559
8. Oh SH, Kauffmann Y, Scheu C, Kaplan WD, Rühle M (2005) Science 310:661
9. Wulff G (1901) Z Krystallogr Mineral 34:449
10. Herring C (1954) Phys Rev 82:87
11. Choi JH, Kim DY, Hockey BJ, Wiederhorn SM, Handwerker CA, Blendell JE, Carter WC, Roosen AR (1997) J Am Ceram Soc 80:62
12. Kitayama M, Glaeser AM (2002) J Am Ceram Soc 85:611
13. Kitayama M, Narushima T, Glaeser AM (2000) J Am Ceram Soc 83:2572
14. Manassidis I, Gillan MJ (1994) J Am Ceram Soc 77:335
15. Huth M, Ritley KA, Oster J, Dosch H, Adrian H (2002) Adv Funct Mater 12:333
16. Ramamurthy S, Hebert BC, Carter CB (1995) Phil Mag Lett 72:269
17. Shaw TM, Duncombe PR (1991) J Am Ceram Soc 74:2495
18. Simpson YK, Carter CB (1990) J Am Ceram Soc 73:2391
19. Susnitzky DW, Carter CB (1992) J Am Ceram Soc 75:2463
20. Mallamaci MP, Carter CB (1998) Acta Mater 46:2895
21. Heffelfinger JR, Carter CB (1997) Surf Sci 389:188
22. Oster J, Kallmayer M, Wiehl L, Elmers HJ, Adrian H, Porrati F, Huth M (2005) J Appl Phys 97:014303
23. Heffelfinger JR, Bench MW, Carter CB (1995) Surf Sci 343:L1161
24. Dorsey PC, Chrisey DB, Horwitz JS, Lubitz P, Auyeung RCY (1994) IEEE Trans Magn 30:4512
25. Matsuoka T, Hagiwara E (2001) Phys Status Solidi A Appl Res 188:485
26. Stampe PA, Bullock M, Tucker WP, Kennedy RJ (1999) J Phys D Appl Phys 32:1778
27. Oster J, Huth M, Wiehl L, Adrian H (2004) J Magn Magn Mater 272–276:1588
28. Chatain D, Chabert F, Ghetta V, Fouletier J (1993) J Am Ceram Soc 76:1568
29. Levi G, Kaplan WD (2003) Acta Mater 51:2793
30. Sadan H, Kaplan WD (2005) J Mater Sci (accepted)
31. Blendell JE, Carter WC, Handwerker CA (1999) J Am Ceram Soc 82:1889
32. Heremann G, Gleiter H, Baro G (1975) Acta Metal 24:353
33. Saylor DM, Rohrer GS, Mason DE, (1999) Proceedings of the international conference on textures of materials, 12th, Montreal QC, Canada, Aug. 9–13, 1999. 2:1637
34. Dingley DJ, Randle V (1992) J Mater Sci 27:4545
35. Dingley D (2004) J Microsc 213:214
36. Sivel VGM, van den Brand J, Wang WR, Mohdadi H, Tichelaar FD, Alkemade PFA, Zandbergen HW (2004) J Microsc 214:237
37. Reyntjens S, Puers R (2001) J Micromech Microeng 11:287